Real-time alignment and reconstruction: performance and recent developments at the LHCb experiment

Agnieszka Dziurda[1], **Lucia Grillo**[2], **Francesco Polci**[3], **Michael Sokoloff**[4]

[1] European Organization for Nuclear Research (CERN), Geneva, Switzerland
[2] University of Manchester, Manchester, United Kingdom
[3] LPNHE, Paris, France
[4] University of Cincinnati, Cincinnati, OH, United States

E-mail: lucia.grillo@cern.ch

Abstract. The LHCb detector is a single-arm forward spectrometer designed for the efficient reconstruction decays of c- and b-hadrons. LHCb has introduced a novel real-time detector alignment and calibration strategy for LHC Run II. Data collected at the start of the fill are processed in a few minutes and used to update the alignment, while the calibration constants are evaluated for each run. This is one of the key elements which allow the reconstruction quality of the software trigger in Run-II, which fully includes the particle identification selection criteria, to be as good as the offline quality of Run-I. This approach greatly increases the efficiency, in particular for the selection of charm and strange hadron decays. We discuss strategy and performance of this novel approach, followed by a presentation of the recent developments implemented for the 2017 run of data taking, and with the performance and reconstruction quality achieved by the LHCb experiment in LHC Run-II.

1. Introduction

The LHCb detector [1][2] is a single-arm forward spectrometer covering the pseudorapidity range $2 < \eta < 5$, designed for the study of beauty and charm hadron decays with special attention to CP violating phenomena as well as searches for physics beyond the Standard Model through rare decays. The detector includes a high-precision tracking system consisting of a silicon-strip vertex detector (VELO) surrounding the pp interaction region [3], a large-area silicon-strip detector (TT) located upstream of a dipole magnet with a bending power of about 4 Tm, and three stations, indicated as T stations (T1-T3 in Fig. 1) of silicon-strip detectors (IT) in the region closer to the beam pipe and straw drift tubes (OT) [4] in the outer region, placed downstream of the magnet. The particle identification system is composed of two ring-imaging Cherenkov detectors (RICH1, RICH2)[5], electromagnetic (ECAL) and hadronic (HCAL) calorimeter, and a system of muon chambers (M1-M5 in Fig. 1)[6]. A schematic view of the LHCb detector and its sub-systems is shown in Fig. 1.

In Run-II (2015-2018) of data taking the LHCb experiment collects data with the bunch crossing rate of 30 MHz. The hardware trigger, based on information from the calorimeter system and muon chambers, reduces the rate of accepted candidates to about 1 MHz, at which the full detector can be read out. The candidates accepted by this stage are processed by the high-level software trigger, with two split stages (HLT1 and HLT2). The real-time reconstruction needs to be achieved within 35 (650) ms in the HLT1 (HLT2). All events passing the first stage are

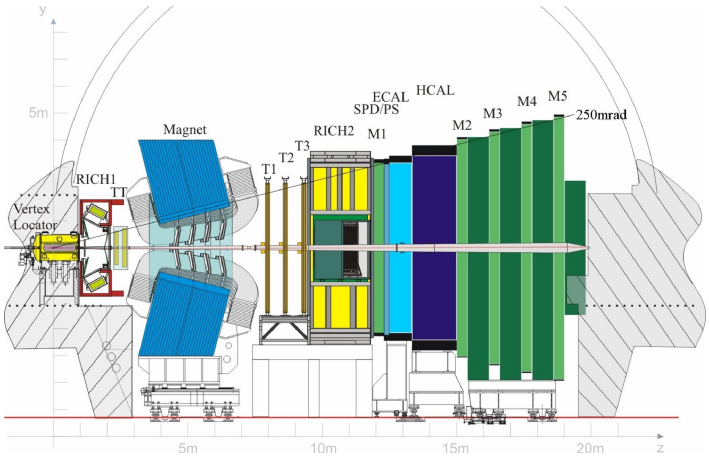

Figure 1. Schematic view of the LHCb detector. The Vertex Locator indicates the vertex detector (VELO). The labels RICH1 and RICH2 denote the Ring Imaging Cherenkov detectors, TT and T1-T3 are the tracking stations, the latter composed of IT and OT detectors in the inner and outer region respectively, M1-M5 indicate the muon chambers, SPD (PS) is the scintillator pad (preshower) detector. ECAL and HCAL mark the electromagnetic and hadronic calorimeters, respectively.

buffered on the Event Filter Farm (EFF). Once available, a fraction of these events is used for the run-by-run real-time alignment and calibrations of the detector. The detector conditions determined with the alignment and calibration tasks can be used immediately in HLT1 and/or in HLT2, resulting in a full, best performing event reconstruction, exploiting the full detector information, achieved as output of HLT2. The level of reconstruction quality that previously was achieved after the offline processing, in Run-II is achieved at the software trigger level, without any need of further offline processing. Fig. 2 illustrates the event reconstruction and selection strategy used by LHCb in Run-II, including the track and primary vertex (PV) reconstruction algorithms, further explained in Sec.3.

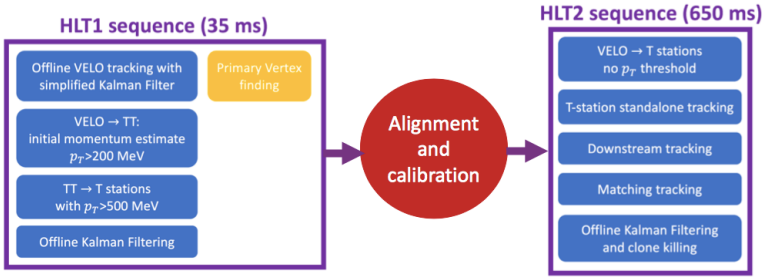

Figure 2. Schematic view of the event reconstruction strategy at LHCb in Run-II. See Sec. 3 for the description of the track and vertex reconstruction algorithms, and Fig. 3 for the track types.

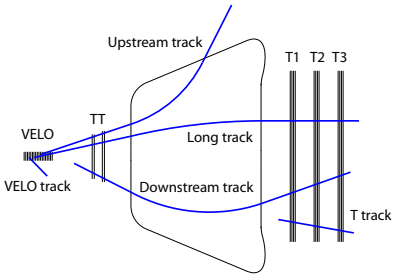

Figure 3. LHCb track types.

2. Real-time alignment and calibration

The spatial alignment of a detector and the accurate calibration of its subcomponents are essential elements to achieve the best physics performance. Pressure and/or temperature changes, together with physical movements either induced by operational conditions, i.e. magnet polarity switch, or mechanical interventions, can modify the position of the detectors and/or their response. The position and orientation of detector elements in the global reference frame must be known with an accuracy significantly better than the single hit resolution. A real-time alignment and calibration procedure is crucial for detector conditions changing with time.

This is particularly important for the VELO, which is retracted and re-inserted for stable beam conditions in each fill to be centred on the primary vertex position in the transverse plane and is therefore sensitive to position changes on fill-by-fill basis. Precise alignment of the VELO is necessary for an accurate identification of primary and secondary vertices, and thus better impact parameter (IP), defined as the minimum distance of a track to a primary vertex, PV, and decay-time resolutions. A more precise alignment of the entire tracking system directly implies a better invariant mass resolution. The time calibration of the OT improves the track reconstruction efficiency in the software trigger [9]. An accurate calibration and alignment of RICH detectors [10] improves the particle identification and allows to increase the sample purity. The calibration of the calorimeter systems [10] is crucial for the energy measurement of neutral particles, affecting the mass resolution of radiative b-hadron decays. The information from the first two stations of the muon system is used to estimate the momentum of the muons passing through the detector, used in the hardware trigger. To guarantee high trigger efficiency without a significant charge asymmetry, an alignment precision better than 1 mm is required.
The alignment of the tracking system uses an iterative procedure of minimizing the residuals of a Kalman filter and takes into account multiple scattering, energy loss in the material and magnetic field information [11]. The usage of primary vertex and mass constraints minimizes global distortions [12]. The alignment and calibrations are performed at regular intervals, which can be at the beginning of the run, fill or less frequently. The resulting constants are updated only if they differ significantly from the constants used to take data. Automatic monitoring procedures are used to make sure the variation of the constants is always within the expected range, and is stable during the fill. Each automatic alignment procedure runs at the start of each fill when the required sample of candidates has been selected, saved in the buffer and reconstructed within the EFF. The VELO alignment is performed first since different beam position with respect to the retractible halves of the VELO directly impact the physics performance of the experiment, the sample needed for the alignment can be collected rapidly and other sub-detectors are aligned relative to the VELO. Figure 4 shows the stability of the tracking system alignment for translations in x and y (VELO), z (Tracker) and x (Muon system, M1-M5 in Fig.1) directions during the first part of 2017 data taking. The horizontal dashed lines indicate the threshold within which the alignment is not updated. Each point denotes the difference between the new constant and the parameter from the previous alignment. The constants are updated every few fills and an overall good stability is found.

3. Real-time track reconstruction

The LHCb tracking system has three main sub-detectors: VELO, TT and T stations. Based on the information from them, several type of tracks can be reconstructed: VELO tracks with hits in the VELO; upstream tracks with hits in the VELO and TT; T tracks with hits in the T stations; downstream tracks with hits in the TT and T stations, which most likely correspond to daughters of long-lived particles. Finally long tracks with hits in at least the VELO and the T stations. Since long tracks are formed using hits before and after the magnetic field, they have the most accurately measured momentum. Due to their properties downstream and long tracks are the most useful for physics analyses. The track types are shown in Fig. 3.
The track reconstruction consists of three main parts. Firstly, the signatures (hits) produced in the detector by charged particles are found and the tracks are formed combining them. Then, all tracks found are fitted using a Kalman filter which obtains the best possible estimate of the true trajectory. This procedure includes corrections due to energy loss and multiple scattering. Finally, duplicated tracks are removed and a container with the best unique tracks is created.
The strict time budget allowed for the reconstruction in HLT1 and HLT2 stages, 35 and 650 ms respectively, requires the usage of different track reconstructions. In HLT1, all VELO tracks are reconstructed and fitted with a simplified Kalman filter. These tracks serve as an input to the

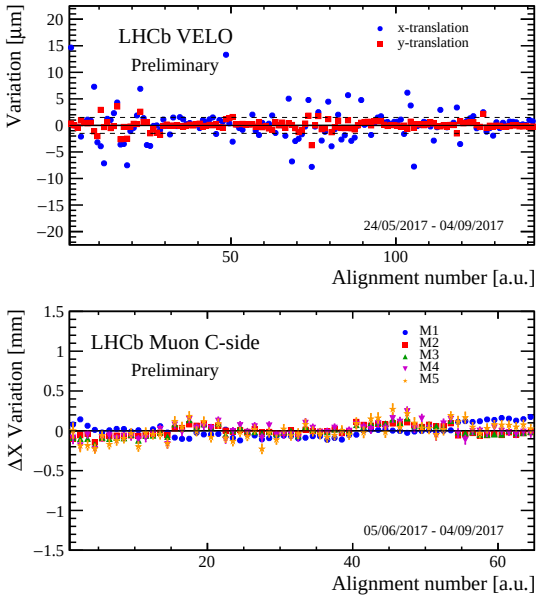

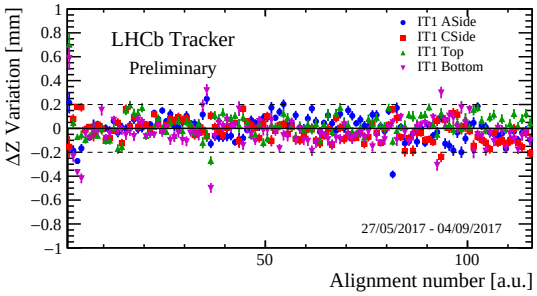

Figure 4. Stability of the alignment constants for VELO (x and y translations), Tracker, IT elements (translation in z direction) and Muon system, right detector side (x translations).

primary vertex finding, some of them are extended to the TT stations creating upstream tracks with an initial momentum estimation. The upstream tracks are extended further to long tracks by looking for hits in the T stations. The resulting long tracks are Kalman filtered and selected with a transverse momentum threshold above 500 MeV/c. They serve as the necessary input to most of the calibration and alignment algorithms. The second stage, HLT2, runs with looser requirements. The VELO or upstream tracks are extended further to long tracks by looking for hits in the T stations, this time without a transverse momentum threshold as well as without requiring clusters in the TT. In addition, T tracks are reconstructed and combined with VELO tracks (long tracks) or with clusters in TT (downstream tracks). All track candidates are fitted with a Kalman filter and clones from different algorithms are removed.

The LHCb experiment intensively uses machine learning in the tracking algorithms. Neural networks are used in the forward tracking (responsible for finding long tracks by extending upstream or VELO tracks) [7] as well as a dedicated fake track rejection algorithm [8]. In 2017 a new tuning for the downstream tracking has been performed exploiting two different multivariate techniques. Firstly, the algorithm filters T tracks using a bonsai Boosted Decision Tree with 11 dimensional discretized space improving the fake T tracks rejection. Then the remaining T track candidates are matched with TT hits. Finally, the good track candidates are selected based on a neural network decision. Overall signal efficiency improvement of about O(3 - 5%) has been found, together with O(3 - 5%) fake reduction.

4. Performance

Excellent reconstruction performance is achieved as shown in Fig 5 - 8. A decay-time resolution of about 45 fs is found for a 4-track vertex. The primary vertex resolution for 25 tracks in z direction is estimated to be 77 μm, while the impact parameter resolution in the x direction is 13 μm for tracks with high transverse momentum. An average tracking efficiency larger than 96% is achieved. In all the relevant physical quantities, the reconstruction performance achieved by LHCb in Run-II at trigger level is comparable or better than the performance of the offline reconstruction in Run-I.

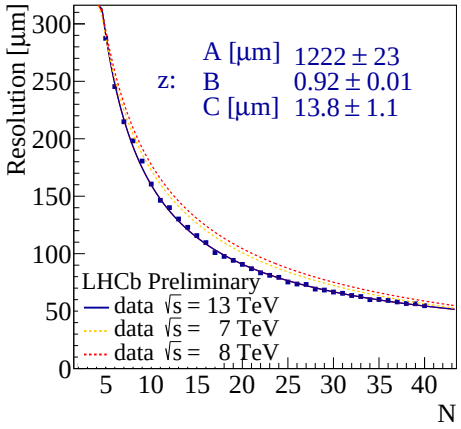

Figure 5. PV resolution along the beam axis (z) versus number of tracks used. Data at $\sqrt{s} = 7$ and 8 TeV collected in Run-I, in 2011 and 2012 respectively are compared to the Run-II, $\sqrt{s} = 13$ TeV dataset.

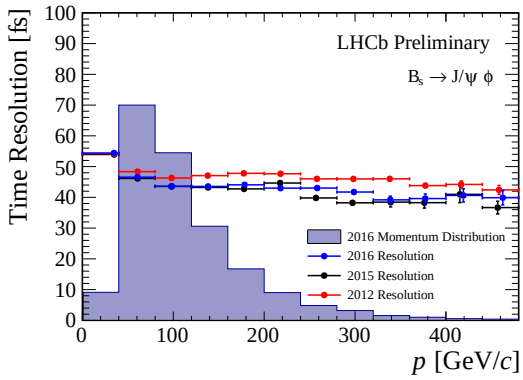

Figure 7. Decay-time resolution for decays with a 4-track secondary vertex as function of momentum. The Run-II datasets (2015 and 2016) are compared to Run-I (2012).

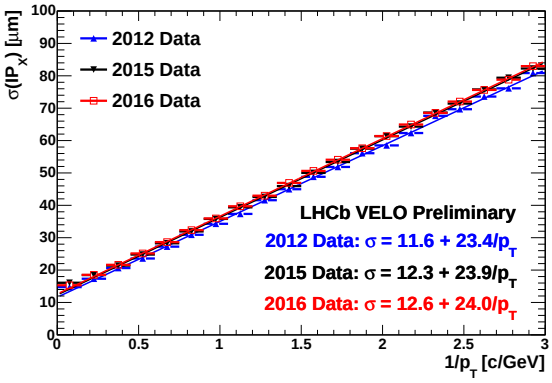

Figure 6. IP resolution as function of the inverse of the transverse momentum. The Run-I dataset has been collected in 2012 while separate Run-II datasets acquired in 2015 and 2016 are compared.

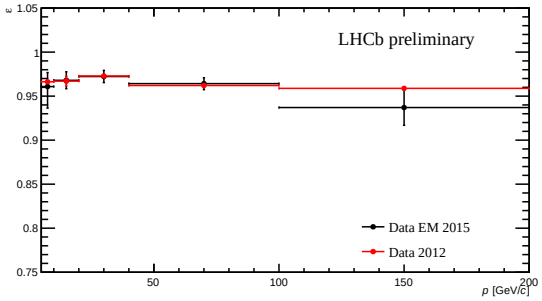

Figure 8. Long track (see Fig 3) reconstruction efficiency as function of the momentum of the track. Performance on data acquired in the first period of Run-II (Data EM) is compared to the Run-I performance. The method is described in Ref. [13]

5. References

[1] Alves Jr. A. A. *et al.* (LHCb collaboration), *JINST* **3** (2008) S08005
[2] Aaij R. *et al.* (LHCb collaboration), *Int. J. Mod. Phys* A **30** (2015) 1530022, arXiv:1412.6352
[3] Aaij R. *et al.* (LHCb VELO group), *JINST* **9** (2014) P09007, arXiv:1405.7808
[4] Arink R. *et al.* (LHCb Outer Tracker group), *JINST* **9** (2014) P01002, arXiv:1311.3893
[5] Adinolfi M. *et al.* (LHCb RICH group), *Eur. Phys. J.* C **73** (2013) 2431 arXiv:1211.6759
[6] Alves Jr. A. A. *et al.*, *JINST* **8** (2013) P02022, arXiv:1211.1346
[7] Stahl M., LHCb-PROC-2017-013, CERN-LHCb-PROC-2017-013.
[8] Seyfert P. *et al*, LHCb-PUB-2017-011.
[9] d'Argent Ph. *et al.* (LHCb Outer Tracker group), *JINST* **12** (2017) no.11, P11016, arXiv:1708.00819
[10] Borghi S., *Nucl. Instrum. Meth. A*, A **845** (2017) 560-564, https://doi.org/10.1016/j.nima.2016.06.050
[11] Hulsbergen W., *Nucl. Instrum. Meth.* A **600** (2009) 471 - 477, arXiv:0810.2241
[12] Amoraal J. , *et al.*, *Nucl. Instrum. Meth.* A **712** (2013), 48-55 arXiv:1207.4756
[13] Aaij R. *et al.* (LHCb collaboration), *JINST* **10** (2015) P02007, arXiv:1408.1251